7. G. M. Oreper, "Motion and solution of a drop in a current-carrying fluid," Inzh.-Fiz. Zh., 28, No. 4 (1975).
8. G. A. Aksel'rud and G. M. Oreper, "Mass transfer between a solid spherical body and a current-carrying fluid," Inzh.-Fiz. Zh., 27, No. 6 (1974).
9. C. Y. Chow and D. F. Billing, "Current-carrying fluid past a nonconducting sphere at low Reynolds number," Phys. Fluids, 10, No. 4 (1967).
10. C. Sozou and W. M. Pickering, "Magnetohydrodynamic flow due to the discharge of an electric current in a hemispherical container," J. Fluid Mech., 73, Part 4 (1976).
11. A. D. Polyanin, "Structure of diffusive wake of an absorbing particle near critical lines," Izv. Akad. Nauk SSSR, Mekh. Zhidk. Gaza, No. 3 (1977).
12. A. S. Brignell, "Mass transfer from a spherical cap bubble in laminar flow," Chem. Eng. Sci., 29, 135 (1974).
13. A. S. Brignell, "Solute extraction from an internally circulating spherical liquid drop," Int. J. Heat Mass Transfer, 18, 61 (1975).
14. B. I. Brounshtein, A. S. Zheleznyak, and G. A. Fishbein, "Heat and mass transfer in interaction of spherical drops and gas bubbles with a liquid flow," Int. J. Heat Mass Transfer, 13, 963 (1970).

ROLE OF RHEOLOGY IN THE EXTENSION OF POLYMER MELTS BY A CONSTANT FORCE

A. N. Prokunin and N. G. Proskurnina

UDC 532.5:532.135

The uniform extension of an elastic liquid by a constant force is experimentally investigated, and the experiment is compared with theory.

In [1] a system of equations with four rheological constants was written to describe any noninertial uniform extension.* These equations were as follows

$$\frac{1}{\lambda}\frac{d\lambda}{d\tau}+\frac{(\lambda+1)(\lambda^3-1)}{6\lambda^2}\exp(-L)=\Gamma(\tau),$$

$$L=\frac{\beta}{2\lambda^2}(\lambda-1)^2(\lambda^2+4\lambda+1),\quad(\tau=t/\theta;\ \Gamma=\varkappa\theta), \tag{1}$$

$$\sigma=\frac{\sigma'\theta}{\eta}=(1-s)(\lambda^2-\lambda^{-1})+3s\Gamma\exp(L).$$

These equations were derived using the classical potential of the grid theory of high elasticity.

In the extension of a sample by a constant force F, one end is rigidly fixed, and the other moves under the action of F (a diagram is shown in Fig. 1). In this case, the dimensionless stress is

$$\sigma=\sigma_0\frac{p_0}{p},\quad \sigma_0=\frac{\theta F}{\eta p_0}. \tag{2}$$

The expression for the deformation rate under tension is $\Gamma = (1/l)(dl/d\tau)$ [3]. Using the incompressibility conditions for the liquid, $p_0 l_0 = pl$, it may be written in the form

$$\Gamma=-\frac{1}{p}\cdot\frac{dp}{d\tau}. \tag{3}$$

Differentiating Eq. (2) with respect to τ and using Eq. (3), the following result is obtained

*Surface tension was neglected.

Institute of Mechanics Problems, Moscow. Translated from Inzhenerno-Fizicheskii Zhurnal, Vol. 36, No. 3, pp. 504-511, March, 1979. Original article submitted January 11, 1978.

 0022-0841/79/3603-0340$07.50

$$\Gamma = \frac{1}{\sigma} \cdot \frac{d\sigma}{d\tau}. \tag{4}$$

Taking account of Eq. (4), the second relation in Eq. (1) takes the form

$$\frac{d\sigma}{d\tau} = -\frac{\sigma \exp(-L)}{3s}\left[(1-s)\frac{\lambda^3-1}{\lambda} - \sigma\right]. \tag{5}$$

It also follows from Eq. (1) that

$$\frac{d\lambda}{d\tau} = -\lambda \exp(-L)\left\{\frac{(\lambda+1)(\lambda^3-1)}{6\lambda^2} + \frac{1}{3s}\left[(1-s)\frac{\lambda^3-1}{\lambda} - \sigma\right]\right\}. \tag{6}$$

Thus, in considering extension by a constant force F, it is necessary to solve a system of two equations – Eqs. (5) and (6) – under the condition that $\lambda = 1$ and $\sigma = \sigma_0$ when $\tau = 0$.

Dividing Eq. (5) by Eq. (6), the following result is obtained

$$\frac{\lambda}{\sigma} \cdot \frac{d\sigma}{d\lambda} = \frac{1}{3s}\left[(1-s)\frac{\lambda^3-1}{\lambda} - \sigma\right]\left\{\frac{(\lambda+1)(\lambda^3-1)}{6\lambda^2} + \frac{1}{3s}\left[(1-s)\frac{\lambda^3-1}{\lambda} - \sigma\right]\right\}^{-1}. \tag{7}$$

Investigation of the phase picture for Eq. (7) shows that the solution $\sigma(\lambda)$ rises monotonically.

It may be shown that at large λ (at large τ) the solution shrinks to the dependence

$$\sigma = \lambda^2. \tag{8}$$

Taking into account that $\sigma(\lambda)$ is monotonic, Eq. (7) may be written in the form

$$\frac{\lambda}{\sigma} \cdot \frac{d\sigma}{d\lambda} = \frac{\frac{1}{3s}\left[(1-s) - \sigma/\lambda^2\right]}{\frac{1}{6} + \frac{1}{3s}\left[(1-s) - \sigma/\lambda^2\right]} + O(\lambda^{-1}). \tag{9}$$

It follows from the second relation in Eq. (1) that the growth in $\sigma(\lambda)$ is no slower than λ^2. Suppose that σ grows more rapidly than λ^2. It then follows from Eq. (9) that, at large λ, $(\lambda/\sigma)(d\sigma/d\lambda) \approx 1$ and $\sigma = C\lambda$, which contradicts the initial assumption. Thus, with increase in λ, all the solutions reduce to a curve $\sigma = C\lambda^2$. It follows from Eq. (9) that $C = 1$.

Taking account of Eq. (8), it follows from Eq. (6) that at large λ

$$\frac{d\lambda}{d\tau} = \frac{\lambda^3}{6}\exp\left(-\frac{\beta\lambda^2}{2}\right). \tag{10}$$

For the case $\beta = 0$

$$\lambda^2 = \frac{3}{C-\tau} = \sigma. \tag{11}$$

Note that λ tends to infinity in a finite time in Eq. (11) because a noninertial approximation is considered; however, in the region of λ considered in the comparison with experiment below, dynamic terms are insignificant, and the asymptote in Eq. (11) is acceptable.

As $\tau \to \infty$ $(\beta \neq 0)$, $\lambda^2 \approx (2/\beta)\ln(\beta\tau/6)$ from Eq. (10); at the same time, the motion of the test sample slows.

In experiments it is not the elastic deformation λ which is measured, but the "elastic recoil" α. The relation between these two quantities [1] is as follows

$$\lambda = \frac{2}{2-s}\alpha^{\frac{2-s}{2(1-s)}} - \frac{s}{2-s}, \quad \alpha = l/l_r. \tag{12}$$

It follows from Eqs. (1) and (10) that, when $\lambda \to \infty$, $\Gamma \to \infty$ if $\beta = 0$ and $\Gamma \to 0$ if $\beta \neq 0$.

According to [1], the rate of irreversible deformation is

$$e_p = \Gamma - \frac{d\ln\alpha}{d\tau} = \Gamma\left[1 - \frac{\lambda}{\alpha} \cdot \frac{d\alpha}{d\lambda}\right] + \frac{\lambda}{\alpha} \cdot \frac{d\alpha}{d\lambda} \cdot \frac{(\lambda+1)(\lambda^3-1)}{6\lambda}\exp(-L). \tag{13}$$

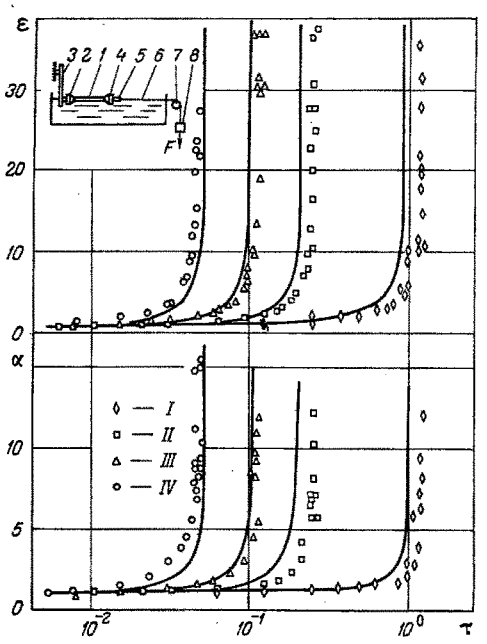

Fig. 1. Uniform extension by a constant force: diagram of extension apparatus; dependence of deformation ε and elastic recoil α on the time τ. Points I–IV correspond to σ_0 = 1.82, 6, 11.4, and 21.3.

If $\beta = 0$ and $\lambda \to \infty$, $(\lambda/\alpha)(d\alpha/d\lambda) \to 2(1-s)/(2-s)$, and $e_p \sim \lambda^2$; if $\beta \neq 0$ and $\lambda \to \infty$, $e_p \to 0$, passing through a maximum.

Now consider the asymptotic solution for small times τ. Substituting into Eqs. (5) and (6) expressions for the total deformation $\varepsilon = l/l_0$, the elastic deformation λ, and the stress $\sigma = \sigma_0 \varepsilon$ in the form of power series in τ, and taking into account that $\Gamma = (1/\varepsilon)(d\varepsilon/d\tau)$, it is found that for any σ_0

$$\varepsilon = \lambda = 1 + \frac{\sigma_0}{3s}\tau + O(\tau^2).$$

It may also be shown that when $\tau < 3s/\sigma_0$, where $\sigma_0 \gg \max(3/2)\{(1-s), s\}$, irreversible flow is slight, i.e., $\varepsilon \approx \lambda$. If $\beta \ll 1$ (for the given polymer $\beta \sim 10^{-2}$)

$$\Gamma = \frac{1}{\lambda} \cdot \frac{d\lambda}{d\tau}; \quad \sigma = \sigma_0\lambda = 3s\,\frac{1}{\lambda} \cdot \frac{d\lambda}{d\tau}, \tag{14}$$

$$\varepsilon \approx \lambda = \frac{1}{1 - \frac{\sigma_0}{3s}\tau}.$$

The expression for ε in Eq. (14) is the same as the solution of the problem on the extension of a Newtonian liquid (F = const) of viscosity ηs, but in the given case the deformation is almost entirely elastic (in a Newtonian liquid $\lambda \equiv 1$).

By matching the asymptotic solutions obtained at large and small τ, the constant C in Eq. (11) may be determined. At the point of intersection of the two solutions, that is, $\sigma = \sigma_0\lambda$ and $\sigma = \lambda^2$ (for the case $\beta \leq 10^{-2}$, the solution for $\beta = 0$ may be considered in the matching region), $\lambda = \sigma_0$. The time τ_* at the matching point may then be determined from Eq. (14)

$$\tau_* = \frac{3s}{\sigma_0}\left(1 - \frac{1}{\sigma_0}\right). \tag{15}$$

Then, substituting $\lambda = \sigma_0$ into Eq. (11) when $\tau = \tau_*$, the following result is obtained

$$C = \tau_* + \frac{3}{\sigma_0^2}. \tag{16}$$

Note that in addition to the asymptotic solution of Eqs. (5) and (6), they were also solved numerically by the Runge–Kutta method on a computer. When the appropriate constraints were observed, the results obtained by the two methods did not greatly differ. The results of the numerical calculation are given below in the comparison with experimental data.

The experiments were carried out, as in [1], at 22°C with a melt of P-20 polyisobutylene of molecular mass $\sim 10^5$.

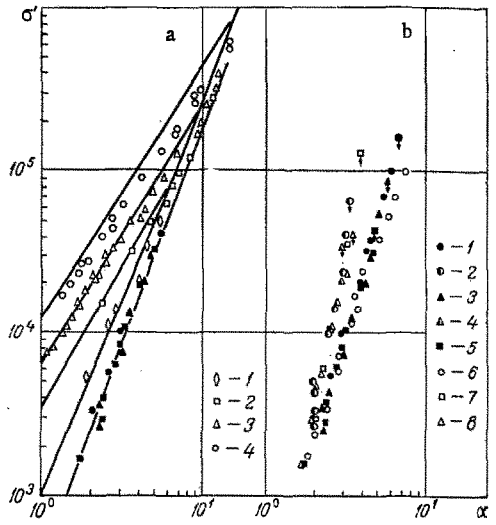

Fig. 2. Dependence of the stress σ' on the elastic deformation α: a) dependence of the tensile stress σ' (Pa) on α. Points 1-4 correspond to σ_0 = 1.82, 6, 11.4, and 21.3. The filled symbols show the envelopes for these dependences; b) the dependence of σ' on α for stress relaxation after extension. Points 1 and 2 correspond to σ_0 = 21.3 and ε = 14, 5.8; points 3 and 4 to σ_0 = 11.4 and ε = 14, 5.8; points 5 to σ_0 = 6 and ε = 14; points 6 show the envelope obtained for extension at a constant deformation rate Γ; points 7 and 8 correspond to extension with constant deformation rates Γ = 200 and 24 and ε = 5.8.

A diagram of the apparatus used for extension by a constant force and for experiments on the stress relaxation of cylindrical samples is shown in Fig. 1. The left-hand end of the sample 1 was fixed by means of the clamp (bush) 2 to the external plate of the capacitative sensor 3 [4]. The right-hand end was fixed by means of another bush 4 to the float 5 on the surface of the water. The water was used to compensate the weight of the sample and to provide thermostatic conditions. A thread 6 was attached to the float, and passed through the pulley 7; the load 8 was attached to its other end. Note that this extension system might lead to self-oscillation at high levels of sample extension (especially when the pulley is replaced by a cylinder over which the thread slides). Therefore, in conditions where this might occur (when the sample weight is much less than the load weight), the experiments were duplicated for vertical extension with no pulley.

For the measurement of stress relaxation, an obstruction was placed at the required distance; the obstruction took the form of a Y piece in which the float lodged in the course of its motion, relaxation beginning thereafter. The sample length remained unchanged in these conditions. In stress relaxation (in ideal relaxation the sample is motionless), the sample may move in the case in which nonuniformities have formed in the course of extension, and this sometimes leads to destruction of the sample. This is evidently because the nonuniformities produce in the sample points of different stress, whose relaxation over time is different.

The uniformity of the samples was partially monitored by taking photographs at a fixed point of the test sample (far from the clamp).

The elastic deformation $\alpha = l/l_r$ was also measured; l_r is the length to which a segment of the extended sample of length l tends after the stress is removed. To measure α, a sufficiently uniform part of the sample was cut out using shears, after which the cut sample was reduced in the melt for ~1 h [3].

In the experiments, measurements were made of the tensile force F, the total deformation $\varepsilon = l/l_0$ (the length l was fixed visually as the melt moved along a scale), and the elastic recoil α.

The scatter of the experimental data for $\varepsilon \leq 10$ was no more than ±10%, but increased dramatically for measurements of ε in the region where it is rapidly rising (see Fig. 1). The points in the figures give the experimental results and the curves the theoretical dependence. For the sake of subsequent comparison with theoretical results, the experimental data are given in dimensionless form.

The dependence of the total deformation $\varepsilon = l/l_0$ and the elastic recoil α on the time $\tau = t/\theta$ ($\theta = 2 \cdot 10^3$ sec) is shown in Fig. 1 for different initial stresses $\sigma_0 = F\theta/\eta p_0$ (p_0 is the cross-sectional area before deformation). In the range of ε investigated, these dependences rise monotonically; the rise is more rapid for larger σ_0.

The dependence of the dimensional stress σ' on the elastic recoil α is shown in Fig. 2. The open symbols in Fig. 2a correspond to results for $\sigma'(\alpha)$ obtained for extension by different forces (initial stresses σ_0'). These dependences are plotted from the experimental results given in Fig. 1. It is evident from Fig. 2 that the experimental dependences $\sigma'(\alpha)$ converge with increase in α. Comparison of results for $\sigma'(\alpha)$ obtained in conditions of constant force (Fig. 2a) and constant deformation rate [1] shows that at the points of intersection the deformation rates are approximately the same.

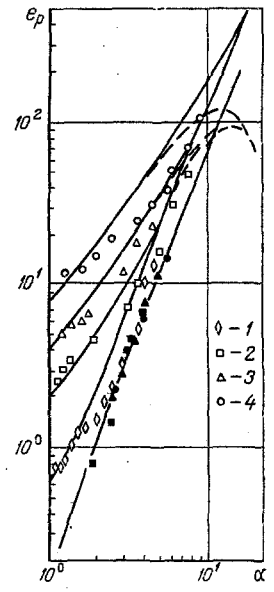

Fig. 3

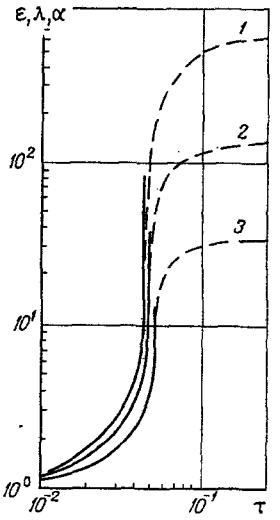

Fig. 4

Fig. 3. Dependence of e_p (1) on the elastic recoil α. Points 1–4 correspond to σ_0 = 1.82, 6, 11.4, and 21.3. The filled symbols show the envelope of the curves for different dependences $e_p(\alpha)$.

Fig. 4. Theoretical dependence of the total deformation ε (1), elastic deformation λ (2), and elastic recoil α (3) on the time τ. The continuous curves are for $\beta = 0$ and the dashed curves for $1.72 \cdot 10^{-3}$.

The filled symbols in Fig. 2a show the dependence $\sigma'(\alpha)$ (the envelope) obtained for stress relaxation. This dependence was obtained as follows. In conditions of stress relaxation (preceded by extension of the sample), measurements were made not only of the stress as a function of time $\sigma'(t)$ but also of the elastic recoil α. The sample was unloaded at different times t in the course of stress relaxation, and the elastic recoil α was measured; the dependence $\alpha(t)$ was then constructed. Using the dependences $\sigma'(t)$ and $\alpha(t)$ in stress relaxation (not given in the present work), the relaxational dependences $\sigma'(\alpha)$ shown by the points in Fig. 2b were obtained. The points from which the relaxation process began are shown by arrows in Fig. 2b. As is evident from Fig. 2b, the relaxation dependences lie along a single curve, if relaxation begins from points lying on this curve (see points 2, 4, 7, and 8, for example). It does not matter in what conditions the points from which relaxation begins (denoted by arrows) were obtained. For example, points 2 and 4 were obtained in conditions of constant force and 7 and 8 in conditions of constant deformation rate. The relaxation curves $\sigma'(\alpha)$ merge in the envelope (6) obtained for relaxation following from extension at constant deformation rate (see [1] and points 6 in Fig. 2b). Thus, the envelopes for these two types of extension are the same.

Note that the dependences $\sigma'(\alpha)$ obtained for extension at constant force (the unfilled symbols in Fig. 2a) lie to the left of the envelope (as is also the case for the dependences for extension at constant deformation rate in [1]).

Dependences $e_p(\alpha) = \Gamma(d\ln\alpha/d\tau)$ for extension with different σ_0 are shown in Fig. 3. The experimental dependences $\varepsilon(\tau)$ and $\alpha(\tau)$ (see Fig. 1) were used to construct $e_p(\alpha)$; in this case, $\Gamma = d\ln\varepsilon/d\tau$. The dependences $e_p(\alpha)$ converge with increase in α. It should be emphasized that here, as for $\sigma(\alpha)$, the envelope (see the filled symbols) is the same as that obtained for extension with constant deformation rate Γ. The procedure for obtaining the envelope in any conditions of extension is given in [1], together with experimental results for the envelope in the case of extension with Γ = const.

At this point, the theoretical and experimental results may be compared. The calculations were made for the constants determined in [1], with the following values: viscosity $\eta \approx 1.1 \cdot 10^6$ Pa · sec; relaxation time $\theta = 2 \cdot 10^3$ sec; ratio of the retardation time to the relaxation time s = 0.35. The continuous curves in the figures correspond to the case $\beta = 0$ and the dashed curves to the case $\beta = 1.72 \cdot 10^{-3}$. No dashed curves appear in

most of the figures because the two variants considered did not differ in the corresponding regions.

The theoretical dependences of the total deformation ε and elastic recoil α on the time τ are calculated from Eqs. (5), (6), and (12). For $\sigma_0 > 10$ and $\varepsilon < 10$, the theoretical curves are little different from the corresponding solution of the problem for a Newtonian liquid in Eq. (14) with viscosity ηs, although in the present case gigantic elastic deformations accumulate (see Fig. 4). Note that the theoretical curves of $\varepsilon(\tau)$ and $\alpha(\tau)$ for $\beta \neq 0$ turn downward after rising sharply; increase in σ_0 is associated with downturn at smaller values of ε. These downturns are not shown in Fig. 1, since, e.g., when $\sigma_0 = 21.3$, the downturn in the curves of $\varepsilon(\tau)$ occurs at $\varepsilon \approx 400$ (see Fig. 4). When $\beta = 0$ the curves of $\varepsilon(\tau)$ and $\alpha(\tau)$ increase without limit.

The theoretical curves of the extension $\sigma'(\alpha)$ shown in Fig. 2a follow from Eq. (1), where Γ is obtained from Eqs. (5) and (6) taking account of Eqs. (4) and (12). Note that $\sigma'(\alpha)$ does not depend on β (for any β). The analytic expression for the envelope is obtained from the expression for σ in Eq. (1) when $\Gamma \equiv 0$, with λ replaced by α in Eq. (12).

The values of e_p (Fig. 3) in extension are calculated from Eq. (13). The analytic expression for the envelope is obtained from Eq. (13) with $\Gamma \equiv 0$. Note that, when $\beta = 0$, e_p increases without limit with rise in α; when $\beta \neq 0$, it has a maximum. It was not possible to confirm the existence of a maximum on the curves of e_p experimentally, because of the difficulty of obtaining large values of α. Such a maximum was obtained in [5] for low-density polyethylene.

It is also interesting to compare the theoretical curves for the total deformation $\varepsilon(\tau)$, the elastic deformation $\lambda(\tau)$, and the elastic recoil $\alpha(\tau)$ shown in Fig. 4 for $\sigma_0 = 21.3$. At small τ, $\varepsilon \approx \lambda$, i.e., the sample medium deforms as a solid nonlinear Voigt body. Note that, in the region where $\lambda \approx \varepsilon$, the elastic recoil α is considerably less than ε. The theoretical curves of $\varepsilon(\tau)$, $\lambda(\tau)$, and $\alpha(\tau)$ for $\beta \neq 0$ turn downward at large τ. The downturn on the theoretical curves of $\varepsilon(\tau)$ for $\beta \neq 0$ shown in Fig. 4 were not experimentally investigated. This is because it is very difficult to achieve values of $\varepsilon \sim 10^2$ experimentally. Curves of $\varepsilon(\tau)$ with a downturn after a sharp rise were observed in [6] for crystallizing polyisobutylene, but at viscosities several orders of magnitude higher than were used in the present work.

NOTATION

λ and α, two measures of the longitudinal elastic deformation; Γ and $\varkappa$, dimensionless and dimensional deformation rates; τ and t, dimensionless and dimensional time; θ, relaxation time; s, ratio of the retardation time to the relaxation time ($0 < s < 1$); η, initial (Newtonian viscosity); β, dimensionless coefficient characterizing the flexibility of the macromolecular chains ($0 \leq \beta \leq 1$); σ and σ', dimensionless and dimensional stress in the cross section of the extended sample; F, tensile force; p_0 and p, cross-sectional area of sample at the onset of deformation ($\tau = 0$) and after deformation for time τ; l, length of sample at time τ; l_0 and σ_0, length of sample and stress in it at $\tau = 0$; l_r, length to which a segment of the extended cylindrical sample of length l tends after the removal of the stress as $\tau \to \infty$; ε, total longitudinal deformation.

LITERATURE CITED

1. A. N. Prokunin and N. G. Proskurnina, "Rheology in the extension of polymer liquids," Inzh.-Fiz. Zh., 36, No. 1 (1979).
2. A. I. Leonov, Rheol. Acta, 15, No. 2 (1976).
3. A. I. Leonov, A. N. Prokunin, and G. V. Vinogradov, in: Successes in Polymer Rheology [in Russian], Khimiya, Moscow (1970), p. 40.
4. M. S. Akutin, A. N. Prokunin, N. G. Proskurina, and O. Yu. Sabsai, Mekh. Polim., No. 2, 354 (1977).
5. A. N. Prokunin, Nonlinear Elastic Phenomena in the Extension of Polymer Liquids. Experiment and Theory [in Russian], Preprint No. 104, Institute of Mechanics Problems, Academy of Sciences of the USSR (1978).
6. G. L. Slonimskii, A. A. Askadskii, and V. K. Logvinenko, Mekh. Polim., No. 4, 659 (1967).